Topological and spatial structure in the liquid-water–acetonitrile mixture

Dan L. Bergman and Aatto Laaksonen
Division of Physical Chemistry, Arrhenius Laboratory, Stockholm University, SE-106 91 Stockholm, Sweden
(Received 13 March 1998; revised manuscript received 3 June 1998)

We have studied the structure of the liquid-water–acetonitrile mixture using molecular configurations obtained by molecular dynamics simulation. Spatial distribution functions have been used to analyze the local structures surrounding the molecules. The effective hydrogen-bond definition has been used to study basic hydrogen-bond properties and topological properties of the hydrogen-bond network. The topology of the network depends on the acetonitrile concentration. Up to a critical concentration, there is an infinite network of hydrogen-bonded water molecules. At higher concentrations, the network cannot be supported, and finite water clusters form. In order to characterize the networks and clusters, we have calculated some properties of loops and chains of water molecules. The patterns of hydrogen bonds surrounding the molecules and the size distribution of the clusters have also been calculated. We suggest that this approach can be useful when studying the structure of other liquid mixtures where hydrogen bonds are an important mode of interaction. [S1063-651X(98)04510-3]

PACS number(s): 61.25.Em, 61.20.Qg, 02.70.−c

I. INTRODUCTION

The water–acetonitrile mixture has been studied theoretically and experimentally for some time. Early experimental work focused on thermodynamic properties, whereas more recent work often employs spectroscopic techniques such as NMR, IR, and x-ray and neutron scattering, which give more direct information about microscopic quantities. Among the early workers are Benter, Moolel, and Schneider [1,2], who studied phase separation phenomena. (Phase separation occurs at certain compositions below $T_c = 272$ K.) Morcom and Smith [3], and Moreau and coworkers [4] measured excess enthalpy, volume, viscosity, and dielectric properties. Drawing on this work, Moreau and Douhéret [4] proposed that for $T > T_c$ the system should have three different types of microstructures depending on the acetonitrile mole fraction (x_{MeCN}): In the first region, $0 < x_{\mathrm{MeCN}} < 0.15 - 0.2$, the voids of the water network are progressively filled by acetonitrile molecules without enhancement of the water structure. In the second region, $0.15 - 0.2 < x_{\mathrm{MeCN}} < 0.75 - 0.8$, clusters of water molecules (that is microheterogeneities) form. The exact nature of these clusters is unclear. The third region is reminiscent of the first, in the sense that the structure of the pure acetonitrile system is gradually disrupted by the insertion of water molecules.

Recent IR measurements by Jamroz, Stangret, and Lindgren [5], and Bertie and Lan [6] give a more detailed picture of the microstructure of the system. Jamroz, Stangret, and Lindgren used the OD and CN stretching vibrations to probe the microstructure. They concluded that preferential solvation (i.e., highly nonrandom mixing) occurs in the region $0.1 < x_{\mathrm{MeCN}} < 0.8$. Furthermore, they proposed that chains of water molecules are formed rather than spherical clusters. They also estimated the fraction of hydrogen-bonded acetonitrile molecules as a function of x_{MeCN}.

Bertie and Lan essentially reproduced the results of Jamroz, Stangret, and Lindgren using a different method (calibrated multiple attenuated total reflection spectroscopy). In addition they calculated the fraction of OH groups engaged in hydrogen bonds. They found that the fraction of hydrogen-bonded groups drops below 0.5 when x_{MeCN} exceeds 0.5. From this they concluded that clusters more complex (with more cross links) than linear chains or hexagons are improbable for $x_{\mathrm{MeCN}} > 0.5$. In the region $0.3 < x_{\mathrm{MeCN}} < 0.5$ they found their results to be consistent with complex microheterogeneities.

The present work employs molecular dynamics (MD) simulations to study the microstructure at different acetonitrile concentrations. We have simulated this system previously [7], but the results were inconclusive on a number of points, especially with respect to the nature of the possible microheterogeneities. Recently we have developed an approach that is suitable for the study of molecular pair configurations [8] and hydrogen-bond network topology [9]. Here we use this approach to analyze the microstructure. First we study basic aspects of the liquid structure such as molecular pair configurations and hydrogen-bond dynamics, and then we proceed to properties related to the topology [9–16] of hydrogen-bond networks and water clusters.

II. COMPUTATIONAL METHOD

Jorgensen and Briggs [17] have developed a simple three-site potential for acetonitrile. This potential has been shown to describe the structural and thermodynamical properties of pure acetonitrile well, in spite of the fact that the methyl group is treated as a united atom. We have used this potential together with the extended simple point charge (SPC/E) water potential [18] to carry out several classical MD simulations within the NVT ensemble (see Fig. 1). Five systems with acetonitrile mole fractions (x_{MeCN}) of 0, 0.11, 0.5, 0.89, and 1 have been investigated at $T = 300$ K [19]. (We will refer to the mixture with $x_{\mathrm{MeCN}} = \alpha$ as the α system.)

The MD runs were started from the final configurations of our previous simulations [7]. The systems were first integrated for 0.3 ns to reach equilibrium in the NVT ensemble. Data were then collected during the following 0.1 ns for all systems. To obtain reliable spatial distribution functions for

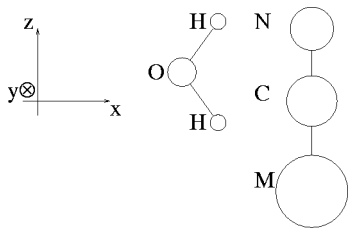

FIG. 1. The geometries of the water and acetonitrile potential models. To the left water with $d_{OH}=1$ Å and HOH$=109.47^{o}$. To the right acetonitrile (N=nitrogen, C=carbon, M=methyl group) with $d_{NC}=1.157$ Å, $d_{CM}=1.458$ Å, and $d_{NM}=2.615$ Å.

the 0.11 and the 0.89 systems, they were simulated an additional 0.7 ns each. Periodic boundary conditions have been applied together with the minimum-image convention [20]. Long-range Coulombic interactions have been evaluated using the Ewald summation technique [21], and the Lorentz-Berthelot combination rules have been used to compute the Lennard-Jones parameters between all types of sites. All simulated systems consisted of 256 molecules and the time step was 1 fs. We have used a modified version of MCMOLDYN [22] to carry out the simulations.

The potential models we have used have been developed mainly for simulation of pure substances. Since we use them for simulations of mixtures, it is important to ascertain that they give reasonable results for some experimentally accessible quantities. We have therefore calculated the diffusion coefficients D and the internal energy E (see Table I). The diffusion coefficients are consistently smaller than the experimental values (except in the pure water system). Especially for the systems with high acetonitrile content, we obtain smaller water diffusion coefficients D_{H_2O} than the experimentalists. The main cause for this is probably the large effective charges on the water molecule, which have been chosen to reproduce the properties of pure water. It is therefore probable that our system is overly structured. However, qualitatively we reproduce the diffusion coefficients' dependence on x_{MeCN}: D_{MeCN} increases monotonously and D_{H_2O} has a local minimum.

As Berendsen, Grigera, and Straatsma [18] have pointed out, one should account for the self-energy associated with the induced dipole moment when the SPC/E model is used. We account for the self energy by increasing the internal energy per molecule by

$$E_{self}=5.23(1-x_{MeCN}), \tag{1}$$

TABLE I. Internal energy E and diffusion coefficients D.

			$D(10^{-9}$ m^2/s)			
	E (kJ/mol)		Calc.		Expt.[b]	
x_{MeCN}	Calc.	Expt.[a]	H_2O	MeCN	H_2O	MeCN
0.0	40.48±0.04	41.5	2.6±0.1		2.3	
0.11	39.60±0.03	40.1	2.1±0.1	1.5±0.1	2.1	1.8
0.5	34.54±0.03	35.3	1.7±0.1	1.9±0.2	3.0	3.3
0.89	30.33±0.04	31.5	2.0±0.3	2.2±0.1	4.9	4.1
1.0	29.70±0.02	31.0		2.7±0.1		4.3

[a]References [3,17,18].

[b]Reference [23].

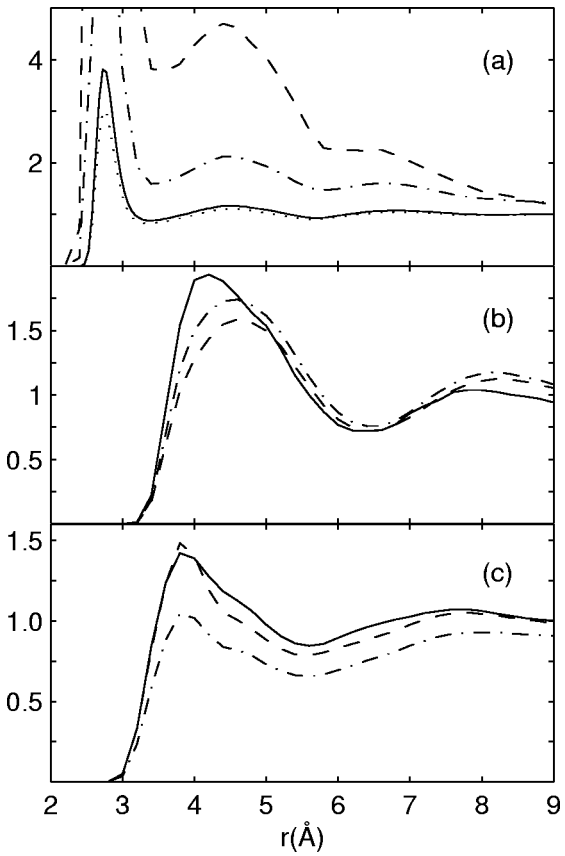

FIG. 2. Radial distribution functions: (a) $g_{OO}(r)$, (b) $g_{CC}(r)$, and (c) $g_{OC}(r)$, for $x_{MeCN}=0$ (dotted), 0.11 (solid), 0.5 (dot-dashed), 0.89 (dashed), and 1.0 (dashed). Note that the 0.89 and 1.0 $g_{CC}(r)$ curves coincide.

where 5.23 kJ/mol is the correction appropriate for pure SPC/E water. This simple correction does not account completely for the self energies, but it should at least reduce the error due to the water molecules.

Directed graphs of hydrogen bonds have been constructed from the simulation trajectories every 5 fs, using the effective hydrogen bond definition(see Sec. IV). In total 2×10^4 graphs have been generated for each system. From these graphs, the hydrogen-bond distributions and some properties of loops and chains have been calculated using TOP-PACK [24]. The periodic boundaries of the simulation box introduce some unphysical loops. By keeping track of the crossing of periodic planes, we have eliminated such loops from the calculations.

III. LOCAL SPATIAL STRUCTURE

Visual inspection of snapshots from the simulations leaves one with the general impression that the water molecules are strongly attracted to each other: At all compositions they tend to form clusters from which the acetonitrile molecules are expelled. The characteristics of these clusters vary with the composition and it is nontrivial to characterize them in a useful way. One traditional approach is based on radial distribution functions of atomic number densities (RDF's). The oxygen-oxygen (OO), carbon-carbon (CC), and oxygen-carbon (OC) distributions are shown in Fig. 2. The OO distributions show clearly how the water molecules

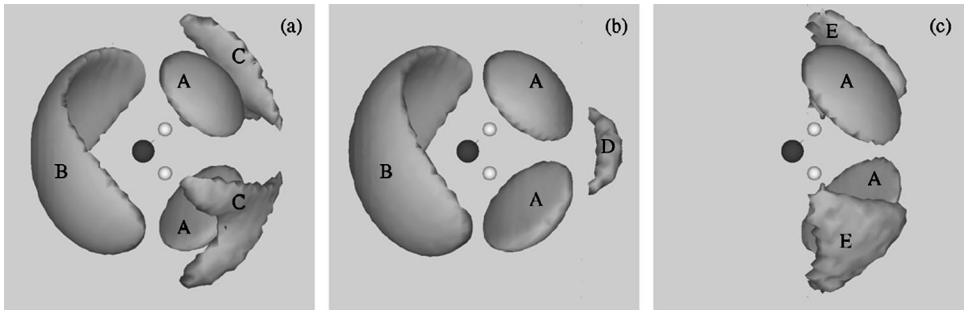

FIG. 3. Spatial distribution functions: The isodensity surfaces (a) $g_{OO}(\boldsymbol{r})=1.5$ for $x_{MeCN}=0$, (b) $g_{OO}(\boldsymbol{r})=11$ for $x_{MeCN}=0.89$, and (c) $g_{ON}(\boldsymbol{r})=1.5$ for $x_{MeCN}=0.11$. The maxima A are due to hydrogen bonds where the central water molecule donates a proton. The maximum B is due to hydrogen bonds where the central water molecule accepts protons. As x_{MeCN} increases, the nontetrahedral features marked by C in (a) are gradually shifted towards D in (b). For $x_{MeCN}>0.11$, the E maxima disappear. See Table II for details concerning the maxima.

tend to form clusters in the 0.50 and 0.89 systems. Despite the rapid increase in the maximum of $g_{OO}(r)$ with x_{MeCN}, the average number of oxygen atoms n in the first coordination shell decreases ($n=4.5$, 4.3, 3.7, and 2.2 for $x_{MeCN}=0$, 0.11, 0.5, and 0.89 respectively). The CC distribution changes less dramatically with composition, but in the 0.11 system the relatively high first peak and the low value at 9 Å is consistent with a pure water region and a region with enhanced acetonitrile content. The low peaks in the OC distributions support this interpretation of the OO and CC distributions.

We have proposed that spatial distribution functions (SDF's) can serve as a natural starting point for the analysis of spatial structure in liquid mixtures [8]. In Figs. 3(a) and 3(b), the maxima marked by A correspond to hydrogen-bond sites where the central water molecule donates a proton, and the maximum B is due to hydrogen bonds where the central water molecule accepts protons. The average number of hydrogen bonds can be estimated as four times the average number found in a maximum of type A. We have obtained 3.3, 3.1, 2.7, and 1.9 for $x_{MeCN}=0$, 0.11, 0.5, and 0.89 respectively, which is lower than the average coordination numbers obtained from the radial distribution functions above.

In pure water we have observed two maxima at nontetrahedral positions [see Fig. 3(a)]. These maxima have been proposed to account for most of the extra 0.5 neighbors of water [25]. We have estimated the average number of oxygen atoms in these maxima to be 0.4. As the concentration of acetonitrile increases, the average number of oxygen atoms in the maxima decreases (see Table II). They are also gradually shifted from position C to position D. However, the mass in the maxima depends strongly on the g_c value used to define them (see Sec. IV below). The significant observation is therefore that the mass decreases and that the position is shifted.

The oxygen-nitrogen distribution is shown in Fig. 3(c) for the water rich 0.11 system. The tetrahedral A maxima, which correspond to hydrogen-bonded nitrogen atoms, are present at all acetonitrile concentrations. The average number of nitrogen atoms found in these maxima increases with x_{MeCN} (see Table II). The nontetrahedral E maxima are only present in the water-rich 0.11 system.

The fact that the two small maxima at the nontetrahedral positions C in the oxygen-oxygen SDF's, move and coalesce at the position D when x_{MeCN} increases; and the fact that we observe maxima for the oxygen-nitrogen SDF at the nontetrahedral positions in the 0.11 system only is consistent with the idea that the pure water and the 0.11 systems consist of networks of water molecules containing some cavities. In these cavities oxygen and nitrogen atoms occasionally reside. At higher acetonitrile concentrations the network changes in character and the cavities disappear. Moreau and Douhéret's original hypothesis embodies this idea [4].

The distributions describing the correlations between acetonitrile molecules are relatively independent of x_{MeCN}; moreover, they are not directly related to the hydrogen-bond structure, hence they are not considered here [26].

IV. DEFINITION AND BASIC PROPERTIES OF HYDROGEN BONDS

A number of different hydrogen-bond definitions are in use and depending on the definition chosen, different results are obtained. Most definitions can be classified either as energetic or geometric [27,28]. We use *the effective hydrogen-bond definition* [8,9]. It is related to the potential of mean force and describes the rearrangement properties of the hydrogen-bond network well.

The oxygen-oxygen SDF, $g_{OO}(\boldsymbol{r})$, has one connected region of high probability V associated with each of its protons [see Figs. 3(a) and 3(b)]. These regions will be called proton donation sites. According to the effective hydrogen-bond definition, a water molecule forms a hydrogen bond to any oxygen atom entering either of these regions. The regions are defined by the relation

$$g_{OO}(\boldsymbol{r})>g_c\,. \tag{2}$$

Similarly, a water molecule forms a bond to any nitrogen atom entering either of the two regions defined by $g_{ON}(\boldsymbol{r})>g_c$ [see Fig. 3(c)]. Note that it is unnecessary to define a proton ''acception'' site behind the water molecules, since one water molecule in each bonded pair donates a proton to the other.

According to the effective hydrogen-bond definition, the average number of oxygen atoms in a hydrogen-bond site is given by

TABLE II. Properties of some SDF maxima. Key: *Atom pair* tells us which distribution function we are dealing with. *Maximum type* corresponds to the notation used in Fig. 3. *CD* denotes a maximum with characteristics intermediate between *C* and *D*. g_c denotes the cut off used to define the connected region surrounding the maximum (see Sec. IV). *Maximum position* ($\mathbf{r}_{\max}$) lists the Cartesian coordinates and the radial coordinate of the point where $g(\mathbf{r})$ has a local maximum. *Maximum height* denotes the value of g at $\mathbf{r}_{max}$. *Mass* denotes the average number of atoms found in the region, see Eq. (3). *Center of mass* has its intuitive meaning. *Bulk average* denotes the mass that would have been found in the region, if the conditional density of atoms surrounding the central molecule was equal to the bulk density of the same atoms. σ is an estimate of the spread (standard deviation) of the mass in the region around its center of mass. $\pm$ indicates that the region contains two maxima one with the + and one with the − coordinate (cf. Fig. 3). Note that all regions in this table are connected. All lengths are in Å.

Atom pair	Maximum type	x_{MeCN}	g_c	Maximum position x	y	z	r	Maximum height	Center of mass x	y	z	r	Mass	Volume	Bulk average	σ
OO	A	0.00	1.0	1.6	0.0	2.2	2.7	53.3	1.6	0.0	2.2	2.8	0.83	4.4	0.15	0.7
OO	A	0.11	1.0	1.6	0.0	2.2	2.7	68.3	1.6	0.0	2.2	2.8	0.78	4.4	0.11	0.7
OO	A	0.50	1.0	1.6	0.0	2.2	2.7	181.0	1.6	0.0	2.2	2.8	0.68	4.4	0.04	0.7
OO	A	0.89	1.0	1.6	0.0	2.2	2.7	878.6	1.6	0.0	2.2	2.8	0.47	4.4	0.006	0.7
OO	A	0.00	2.0	1.6	0.0	2.2	2.7	53.3	1.6	0.0	2.2	2.8	0.75	2.6	0.09	0.6
OO	A	0.11	2.0	1.6	0.0	2.2	2.7	68.3	1.6	0.0	2.2	2.8	0.71	2.6	0.07	0.6
OO	A	0.50	2.0	1.6	0.0	2.2	2.7	181.0	1.6	0.0	2.2	2.8	0.62	2.6	0.02	0.6
OO	A	0.89	2.0	1.6	0.0	2.2	2.7	878.6	1.6	0.0	2.2	2.8	0.44	2.6	0.003	0.6
OO	C	0.00	1.5	2.8	2.2	0.0	3.6	1.7	2.3	2.5	0.0	3.7	0.19	3.7	0.12	1.4
OO	CD	0.11	1.6	3.2	$\pm$1.6	0.0	3.6	1.9	2.8	0.0	0.0	3.7	0.33	7.7	0.19	2.4
OO	CD	0.50	3.2	3.8	$\pm$0.2	0.0	3.8	4.2	3.4	0.0	0.0	3.7	0.11	3.5	0.03	1.5
OO	D	0.89	8.5	3.8	$\pm$0.4	0.0	3.8	13.4	3.6	0.0	0.0	3.8	0.06	4.1	0.006	1.2
ON	A	0.11	1.3	1.8	0.0	2.2	2.8	13.4	1.7	0.0	2.2	3.0	0.06	7.0	0.02	1.0
ON	A	0.50	1.3	1.8	0.0	2.2	2.8	16.6	1.8	0.0	2.2	3.0	0.17	7.0	0.06	1.0
ON	A	0.89	1.3	1.8	0.0	2.2	2.8	29.2	1.8	0.0	2.2	3.0	0.36	7.0	0.08	0.9
ON	A	0.11	2.0	1.8	0.0	2.2	2.8	13.4	1.7	0.0	2.3	3.0	0.05	4.7	0.01	0.9
ON	A	0.50	2.0	1.8	0.0	2.2	2.8	16.6	1.8	0.0	2.2	3.0	0.15	4.7	0.04	0.9
ON	A	0.89	2.0	1.8	0.0	2.2	2.8	29.2	1.8	0.0	2.2	3.0	0.32	4.7	0.05	0.9
ON	E	0.11	1.5	2.0	3.0	0.0	3.6	1.9	1.6	3.2	0.0	3.7	0.02	4.3	0.01	1.1

$$n_{\mathrm{AB}}(V)=\rho_{\mathrm{B}}\int_V g_{\mathrm{AB}}(\mathbf{r})dV, \tag{3}$$

where $n_{\mathrm{AB}}(V)$ is the average number (the mass) of type B atoms found in the the region V defined relative to atoms of type A. ρ_{B} denotes the bulk density of type B atoms.

The average number of hydrogen bonds per molecule depends on the system's acetonitrile concentration. In order to compare the different systems, we have used the same integration region (V) in Eq. (3) for all concentrations. For the HO bonds, we have used $g_{\mathrm{OO}}(\mathbf{r})$ corresponding to the pure water system in Eq. (2) to define V. Similarly, we have used $g_{\mathrm{ON}}(\mathbf{r})$ corresponding to the 0.89 system to define the HN bonds. Two pairs of g_c values, the *relaxed* and the *strict*, have been used to define the hydrogen bonds. The relaxed pair has $g_c=1$ for the HO bonds and $g_c=1.3$ for the HN bonds [29]. The strict pair has $g_c=2$ for the HO bonds and $g_c=2$ for the HN bonds. We have used both pairs of g_c values to demonstrate to what extent our results depend on the g_c value chosen. Nevertheless, we expect the relaxed definition to reflect the rearrangement properties of the mixture better than the strict definition [9].

Since all hydrogen-bond sites are small, the probability that two atoms (OO, ON, or NN) simultaneously occupy the same site is small. When the relaxed definition is used, the fraction of the occupied sites that contains two atoms simultaneously is less than 8.6×10^{-4} in all cases [30]. When the strict definition is used, no overlap is observed.

The exact value of g_c is not important, since the gradient of $g(\mathbf{r})$ is relatively large on the surfaces of the hydrogen-bond sites. If one uses the relaxed pair of g_c values, then the average number of HO bonds increases at most by 0.083 (for the pure water system), and the average number of HN bonds increases at most by 0.041 (for the 0.89 system), compared with the results obtained using the strict pair of g_c values. In these extreme cases the volumes of the hydrogen-bond sites increase by 1.8 Å^3 and 3.3 Å^3, respectively (see Table II).

In general, the shape of the regions defined by $g(\mathbf{r})>g_c$ changes when $g(\mathbf{r})$ for different acetonitrile concentrations are used. We have used the hydrogen-bond sites [that is the regions obtained using $g_{\mathrm{OO}}(\mathbf{r})$ for the pure water and $g_{\mathrm{ON}}(\mathbf{r})$ for the 0.89 system] regardless of the acetonitrile concentration. To estimate the robustness of this approach, we have calculated the minimum value g_m that $g(\mathbf{r})$ takes in the hydrogen-bond sites. Then the relation $g(\mathbf{r})>g_m$ has been

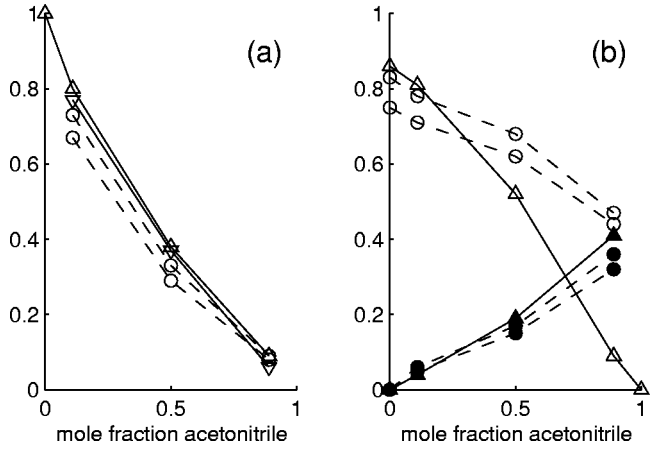

FIG. 4. (a) The fraction acetonitrile molecules engaged in hydrogen bonds, and (b) the fractions of water protons that are engaged in HO bonds (open) and HN bonds (solid). The experimental results are indicated by triangles: the upward tip is from Bertie and Lan [6]; the downward tip is from Jamroz, Stangret, and Lindgren [5]. The simulation results are indicated by circles. Both the relaxed and strict hydrogen-bond definitions have been used. The relaxed definition always gives higher fractions than the strict (see Sec. IV and Table II).

used to define new integration regions. Note that g_m and $g(\boldsymbol{r})$ depend on the acetonitrile concentration. In the case of the relaxed HO hydrogen-bond sites, the volume of the integration region changes less than 1.1 Å^3 and the average number of hydrogen bonds less than 0.02. When we apply this method to the relaxed HN hydrogen-bond sites, the volume of the region changes more. This is caused by the large gradient on the surface. However, the $g_{\mathrm{ON}}(\boldsymbol{r})$ corresponding to different acetonitrile concentrations has similar form near the hydrogen-bond sites, hence the average number of hydrogen bonds is relatively insensitive to the exact shape of the integration region.

The masses, the location, and some other properties of the hydrogen-bond sites are listed in Table II. The fraction of acetonitrile molecules engaged in hydrogen bonds is plotted together with experimental data in Fig. 4(a), and the fractions of hydrogen-bond sites engaged in HO and HN bonds are plotted in Fig. 4(b). The fraction engaged in HO bonds decreases from 0.83 to 0.47 as x_{MeCN} increases from 0 to 0.89. At the same time, the fraction of the sites engaged in HN bonds increases from 0.06 to 0.36, and the total fraction of hydrogen bonds thus remains between 0.83 and 0.85 at all compositions. The fractions of occupied sites depend on the g_c value used to define the hydrogen bonds, but the observed trends remain the same.

Jamroz, Stangret, and Lindgren [5] and Bertie and Lan [6] have estimated the fraction of hydrogen bonds from IR experiments and they have obtained results similar to ours for the fraction of hydrogen-bonded nitrogen atoms [see Fig. 4(a)]. Bertie and Lan have also estimated the fractions of water protons that engages in HN and HO bonds. At high acetonitrile concentrations, they have obtained lower values than we for the fraction of HO bonds [see Fig. 4(b)]. The total fraction of water molecules engaged in hydrogen bonds thus decreases from 0.85 to 0.5 in the measurements of Bertie and Lan. There are several possible causes of the discrepancy between their and our results. The imperfect representation of the dependence of the water molecule's polarization on x_{MeCN} being one. It can yield a too strong HO bond for large x_{MeCN}.

TABLE III. Average lifetimes τ of HO and HN bonds.

x_{MeCN}	HO τ (ps)	HN τ (ps)
0.0	2.11±0.03	
0.11	2.32±0.03	0.99±0.04
0.50	2.93±0.20	1.17±0.04
0.89	6.43±0.48	1.51±0.06

V. LIFETIMES AND TRANSITION PROBABILITIES

A basic understanding of the dynamics of the system can be obtained by studying the formation and duration of different types of hydrogen bonds. We have estimated the lifetimes of the HO and HN bonds and the rates at which the different atom types replace each other on hydrogen-bond sites. The lifetime τ of a hydrogen bond is defined as the time period that begins when an oxygen or nitrogen atom enters a hydrogen-bond site. The time period ends when another atom enters the site. Since two atoms cannot coexist in the site [31], the original atom must have left before the second atom entered. Note that the hydrogen bond is not terminated just because the original atom leaves the site. The lifetimes obtained in this way may thus include time periods when the site is empty, and they should therefore be considered as upper bounds. Since each site is occupied at least 75% [32] of the time, the overestimation should be less than about 33% [33]. The lifetimes are listed in Table III. We see that the average lifetime of the HN bond increases from 0.99 ps to 1.51 ps. The average lifetime of the HO bond increases from 2.11 ps to 6.43 ps. The average lifetime of HO bonds is thus longer than that of HN bonds at all studied compositions, and the longest lifetime by far is found for the HO bonds in the 0.89 system.

In order to gain some insight into how hydrogen bonds form and break, we have estimated the transition probability $\pi_{\mathrm{A}\to\mathrm{B}}$, that is, the number of times that an atom of type B replaces an atom of type A on a hydrogen-bond site per picosecond. To obtain $\pi_{\mathrm{A}\to\mathrm{B}}$, we have divided the total number of transitions from A to B by the number of hydrogen-bond sites (the number of water molecules times two), by the length of the time period, and by the fraction of the time period that a hydrogen-bond site is occupied by an atom of type A. The transition probabilities are shown in Table IV. It can be seen that the rate at which oxygen atoms replace oxygen atoms $\pi_{\mathrm{O}\to\mathrm{O}}$ falls from 0.63 ps^{-1} in the pure water system to 0.10 ps^{-1} in the 0.89 system. Similarly, $\pi_{\mathrm{N}\to\mathrm{O}}$ falls from 0.96 ps^{-1} in the 0.11 system to 0.13 ps^{-1} in the 0.89 system. $\pi_{\mathrm{O}\to\mathrm{N}}$, on the other hand, does not change significantly with the acetonitrile concentration.

It appears that the increasing lifetimes in general, and the long lifetime of the HO bonds at x_{MeCN} in particular, are (at least partly) due to the low water fraction: In pure water, there are a number of water molecules close to every hydro-

TABLE IV. Transition probabilities π. $\pi_{A\to B}$ denotes the number of times that an atom of type B replaces an atom of type A on an *occupied* hydrogen-bond site per picosecond.

x_{MeCN}	$\pi_{O\to O}$	$\pi_{O\to N}$	$\pi_{N\to O}$	$\pi_{N\to N}$
0.0	0.63			
0.11	0.50	0.07	0.96	0.61
0.50	0.31	0.11	0.47	0.88
0.89	0.10	0.09	0.13	0.89

gen bond. These molecules can replace either of the two original molecules, should the hydrogen bond during some fluctuation expose this possibility. At lower water concentrations this mechanism is suppressed by the scarcity of water molecules in reasonable positions (cf. $\pi_{O\to O}$ and $\pi_{N\to O}$ in Table III). One may also note that $\pi_{O\to N}$ does not increase with the acetonitrile concentration.

VI. HYDROGEN-BOND DISTRIBUTIONS

One basic aspect of the hydrogen-bond network is the probability distribution describing the number and types of hydrogen bonds that a water molecule is engaged in with other *water* molecules. Using the hydrogen-bond sites already introduced, we can determine how many protons a given water molecule donates to form hydrogen bonds. The water molecule is said to accept binding protons if any other molecule donates protons to it. Thus, according to this definition, each water molecule can form between 0 and 5 hydrogen bonds. In principle, a water molecule could accept more than three binding protons, but this never happens in our simulations; it is improbable to accept three protons already. The probabilities are 0.046, 0.030, 0.011, and 0.002 for $x_{MeCN}=0$, 0.11, 0.5, and 0.89, respectively, when the relaxed hydrogen-bond definition is applied. The probability distributions describing the fractions of water molecules with different hydrogen-bond configurations are given in Table V.

In pure water, the state corresponding to accepting two and donating two protons is the most common. As anticipated, the average number of HO bonds that the water molecules engages in decreases when the acetonitrile concentration increases. Gradually, the probability mass is transferred to the states that correspond to accepting zero or one and donating zero or one protons; the hydrogen-bond network is gradually depleted of cross links as the acetonitrile concentration increases. In the 0.89 system, we expect linear arrangements of water molecules to dominate.

One can estimate the correlation between the different hydrogen bonds by taking the product of the marginal distributions in Table V. At high acetonitrile concentration, the state corresponding to accepting zero and donating two protons and the state corresponding to accepting two and donating zero protons are assigned higher probability by the product distribution than by the full distribution. This indicates that donation and acception of protons are correlated in such

TABLE V. The probability distribution for the different states of the water molecule estimated from the simulation. The states are defined by the number of protons donated and accepted. Note that only donation of protons to other water molecules is considered. The pairs 00, 01, 10, and 11 describe the two donor sites. 1 indicates that the donor is engaged in a hydrogen bond and 0 the opposite. The 01 and the 10 donor configurations are equivalent. The sums of the probabilities have therefore been listed under 01,10. *Acceptor* denotes the number of protons accepted. Results are given for four different mole fractions of acetonitrile (x_{MeCN}). The estimated standard errors follow the $\pm$ signs. The relaxed hydrogen-bond definition has been used (see Sec. IV).

		Donor		
x_{MeCN}	Acceptor	00	01,10	11
0	0	0.0009±0.0001	0.0054±0.0006	0.0100±0.0005
	1	0.0130±0.0003	0.110±0.002	0.222±0.001
	2	0.0137±0.0005	0.152±0.002	0.427±0.003
	3	0.0006±0.0001	0.0074±0.0004	0.0381±0.0007
0.11	0	0.0012±0.0001	0.0078±0.0003	0.0117±0.0005
	1	0.024±0.001	0.158±0.001	0.237±0.001
	2	0.0185±0.0008	0.169±0.002	0.344±0.003
	3	0.0004±0.0001	0.0072±0.0003	0.0222±0.0009
0.5	0	0.011±0.001	0.024±0.002	0.016±0.001
	1	0.077±0.004	0.259±0.005	0.233±0.003
	2	0.025±0.001	0.147±0.003	0.196±0.006
	3	0.0004±0.0001	0.0038±0.0004	0.0071±0.0004
0.89	0	0.13±0.01	0.060±0.006	0.028±0.005
	1	0.18±0.01	0.287±0.006	0.174±0.006
	2	0.026±0.005	0.060±0.007	0.063±0.004
	3	0.0002±0.0002	0.0007±0.0004	0.0009±0.0004

TABLE VI. Distributions of the number of hydrogen bonds that water molecules in the classes N, NN, O, and OO are engaged in, see the text. Results are given for three different mole fractions of acetonitrile (x_{MeCN}). *Bonds* denotes the number of hydrogen bonds that the molecule is engaged in (not counting the one or two bonds which define the class of the molecule). *Mean* denotes the average number of bonds. *Fraction* denotes the fraction of all water molecules that belong to the class. The tabulated values are based on the relaxed definition of the hydrogen bond (see Sec. IV).

		Class			
x_{MeCN}	Bonds	N	O	NN	OO
0.11	fraction	0.10	0.87	0.0035	0.61
	0	0.00	0.01	0.03	0.02
	1	0.09	0.15	0.48	0.39
	2	0.47	0.42	0.49	0.56
	3	0.42	0.40	0.01	0.04
	4	0.02	0.03		
	mean	2.36	2.29	1.47	1.61
0.5	fraction	0.27	0.66	0.041	0.45
	0	0.02	0.02	0.11	0.04
	1	0.17	0.21	0.71	0.51
	2	0.54	0.46	0.17	0.43
	3	0.27	0.30	0.00	0.02
	4	0.01	0.01		
	mean	2.08	2.08	1.06	1.43
0.89	fraction	0.39	0.41	0.17	0.27
	0	0.13	0.06	0.37	0.11
	1	0.26	0.30	0.54	0.66
	2	0.51	0.48	0.09	0.24
	3	0.10	0.15	0.00	0.00
	4	0.00	0.00		
	mean	1.58	1.74	0.71	1.14

a way that a chain of water molecules tends to have its bonds aligned in the same direction. (A bond points from the water molecule that donates the proton towards the one accepting it.)

In addition to studying the bond distributions of all water molecules, we have looked at the properties of different classes of water molecules. Some of the water molecules donate protons to form hydrogen bonds with one or two acetonitrile molecules. We have studied the following four classes of water molecules in order to see if the presence of such HN bonds coincides with different proton accepting behavior. The classes are (N) water molecules that hydrogen bond to exactly one nitrogen atom, (NN) water molecules that hydrogen bond to exactly two nitrogen atoms, (O) water molecules that donate at least one proton to another water molecule and that do not hydrogen bond to any nitrogen atom, and (OO) water molecules that donate both protons to other water molecules. The fractions of water molecules in the different classes and the distributions of the number of hydrogen bonds that they are engaged in are listed in Table VI. The classes N and O, and NN and OO are suitable for comparison with each other: N and O both have one donor and all acceptor sites free, and NN and OO both have two occupied donor sites and all acceptor sites free.

TABLE VII. The fraction of acetonitrile molecules that hydrogen bond to different numbers of water molecules. The column No. denotes the number of water molecules that the acetonitrile molecule bonds to. The tabulated values are based on the relaxed definition of the hydrogen bond (see Sec. IV).

	Acetonitrile mole fraction		
No.	0.11	0.5	0.89
1	0.583	0.304	0.086
2	0.150	0.024	0.002
3	0.005	0.000	0.000
Sum	0.738	0.328	0.088

In the 0.11 system, the average number of hydrogen bonds is higher for a water molecule that donates exactly one proton to an acetonitrile molecule (class N water), than for a water molecule that donates at least one proton to another water molecule (class O water). It is thus possible for a water molecule to hydrogen bond to an acetonitrile molecule and still be incorporated in the hydrogen-bond network. However, the water molecules that donate two protons to acetonitrile molecules (class NN water) accept on the average fewer binding protons than those that donate two protons to other water molecules (class OO water). For example, the probability that a class NN water molecule accepts two binding protons is lower than the probability that a class OO water molecule does.

For the systems with $x_{MeCN} > 0.11$ there is no network of hydrogen-bonded water molecules extending throughout the whole simulation box. The general trend in these systems is that water molecules with one or two hydrogen bonds to acetonitrile molecules form fewer hydrogen bonds to water molecules. This is no surprise, since water molecules that hydrogen bond to acetonitrile molecules frequently are located in the extreme parts of a water cluster, or in the acetonitrile region.

Another molecular event related to the structure of the hydrogen-bond network is the number of acetonitrile molecules that bind to one, two, or more water molecules simultaneously (see Table VII). Most acetonitrile molecules bind to one or two water molecules. The ratio between the number bonding to one and the number bonding to two increases with the fraction of acetonitrile in the solution. This is not surprising. It is, however, interesting to note that the fraction is relatively large for the 0.11 system: one water molecule out of five bonding to acetonitrile shares its acetonitrile molecule with another water molecule.

VII. NETWORK AND CLUSTER CHARACTERISTICS

At each acetonitrile concentration most water molecules are connected by hydrogen bonds and form one large cluster. The number of molecules in these large clusters fluctuates. A cluster of the most frequently occurring size will be called a maximum-likelihood (ML) cluster. Clusters that differ from their corresponding ML cluster at most by five molecules occur nearly as frequently as the ML cluster. At each acetonitrile concentration, regardless of the hydrogen-bond defini-

TABLE VIII. Properties of the ML clusters. Both the relaxed (r) and the strict (s) hydrogen-bond definition have been used (see Sec. IV). *Configuration fraction* denotes the fraction of the studied configurations that contains the cluster; and e/v denotes the edge-to-vertex ratio.

		Acetonitrile mole fraction			
		0	0.11	0.5	0.89
Cluster size	r	256	228	127	25
	s	255	227	125	22
Configuration fraction	r	0.79	0.75	0.29	0.26
	s	0.36	0.30	0.15	0.17
e/v	r	1.67	1.57	1.37	1.11
	s	1.51	1.44	1.26	1.06

tion used, one cluster of a size within ± 5 molecules of the ML cluster is present in at least 90 percent of the configurations studied. The fraction of water molecules in one and two molecule clusters increases with x_{MeCN}. In the pure water and the 0.11 system, the fraction of water molecules in clusters of this type is at most 0.005. For the 0.5 and the 0.89 systems, the fractions are 0.01 and 0.13 when the relaxed hydrogen-bond definition is used, and 0.02 and 0.14 when the strict definition is used.

In our analysis of the clusters, we have regarded each water molecule as a vertex (v) and each HO bond as an edge (e). The edges are directed, that is they point from the water molecule donating the proton towards the molecule accepting it. The edge-to-vertex ratio (e/v), the frequency, and the size of the ML clusters are listed in Table VIII. The ratio remains essentially unchanged as the cluster size fluctuates around the ML size (within 5% for ± 5 molecules). The e/v ratio for small clusters is nearly minimal: No cluster consisting of less than seven water molecules (except one) contains any loops, thus $v-e=1$. The connectivity of one cluster of the 0.89 system is shown schematically in Fig. 5.

When the acetonitrile concentration in the mixture increases from 0 to 0.89, the edge-to-vertex ratio in the large clusters decreases from 1.67 to 1.11. The lower ratios in the acetonitrile-rich systems are accompanied by a larger number of HN bonds. In the 0.89 system, the low ratio implies that clusters consist mainly of chains and loops (see Fig. 5). The other systems have sufficiently high edge-to-vertex ratios to support networks with more cross links. In the pure water and the 0.11 systems, there is an infinite hydrogen-bond network extending throughout the entire simulation box. The 0.5 and 0.89 systems, cannot support an infinite network; instead one large cluster and a few smaller clusters of water molecules form.

In order to investigate the structure of the hydrogen-bond network further, we have analyzed some properties of the loops and chains of water molecules that make up the clusters. Let us make the following definitions: A *chain* is a connected nonrepeating sequence of edges, and a *loop* is a chain whose ends meet [34]. A *clean* loop is a loop with the additional property that there is no external connecting path between any two vertices in the loop that is shorter than *both* of the two paths that are part of the loop and connect the vertices [13]. We have computed the number of clean loops per water molecule for each of the systems with different acetonitrile content (see Fig. 6).

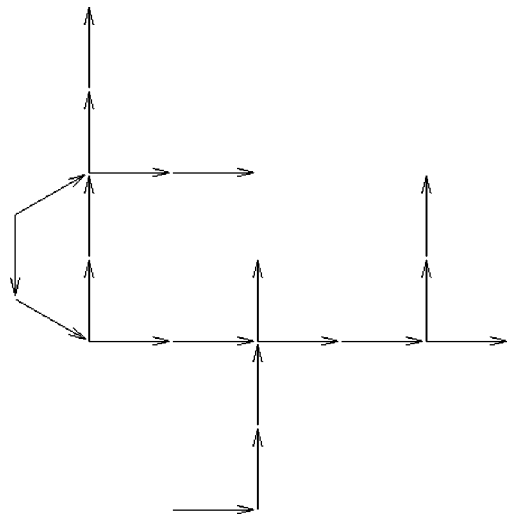

FIG. 5. A schematic representation of a water cluster obtained from the simulation with $x_{\mathrm{MeCN}}=0.89$. Each arrow indicates a hydrogen bond. The arrows point from the water molecule donating the proton towards the one accepting it. The relaxed hydrogen-bond definition has been used (see Sec. IV).

The number of loops of different lengths describes the network structure in all systems. As anticipated, the water-rich systems have more loops of all lengths than the water-depleted systems. Six loops are the most frequent in the pure water and the 0.11 systems. Five loops are the most frequent in the 0.50 and the 0.89 systems. Two mechanisms reducing the number of long loops are short circuiting and low entropy: The longer the loop, the larger the probability that it is short circuited. In the 0.89 and perhaps also in the 0.5 system, long loops are associated with low entropy, since there are few molecular arrangements that give rise to them. (This is not true for the systems with infinite water networks.) The shift of the maximum from six- to five loops can be caused by this entropy effect.

More complete insight into the topology of the hydrogen-

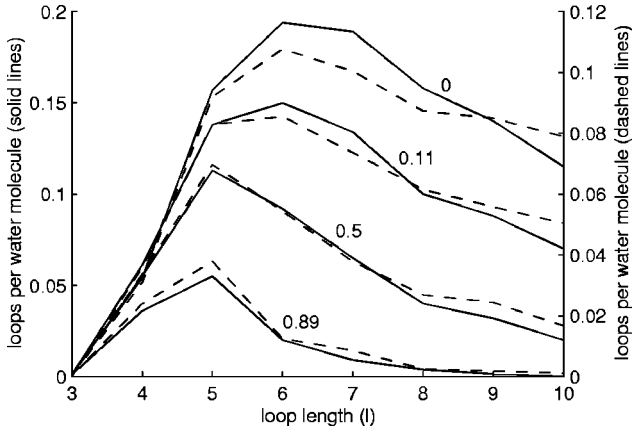

FIG. 6. The number of loops of different lengths l per water molecule for $x_{\mathrm{MeCN}}=0$, 0.11, 0.5, and 0.89. The solid (dashed) lines are based on the relaxed (strict) definition of the hydrogen bond (see Sec. IV).

TABLE IX. The average directionality $\langle d \rangle$ for chains of different length l. The tabulated values are based on the relaxed definition of the hydrogen bond (see Sec. IV). $\langle d \rangle$ changes by less than 0.05 if the strict definition is applied. The standard errors are less than 0.007.

		Simulation			
		Acetonitrile mole fraction			
l	Theory	0.0	0.11	0.5	0.89
2	1.33	1.33	1.34	1.37	1.42
3	1.89	1.88	1.90	1.94	2.01
4	2.07	2.07	2.10	2.16	2.26
5	2.48	2.48	2.51	2.58	2.71
6	2.62	2.62	2.66	2.76	2.90

bond network can be obtained using the ldm scheme [9]. This scheme classifies loops and chains not only according to their length l, but also according to their directionality d and their meeting-point number m. To obtain d one arbitrarily defines one direction along the chain or loop as positive. The directionality is then given by

$$d = |n_+ - n_-|, \tag{4}$$

where n_+ denotes the number of edges pointing in the positive direction and n_- denotes the number of edges pointing in the opposite (negative) direction. The meeting-point number is defined by

$$m = \sup\{m_+, m_-\}, \tag{5}$$

where m_+ denotes the number of vertices with meeting edges and m_- denotes the number of vertices with parting edges. ($m_+ = m_-$ for loops.) In Table IX, the average directionalities $\langle d \rangle$ for chains of different lengths are listed. One can see that $\langle d \rangle$ increases with x_{MeCN}.

A theoretical calculation of the fraction of loops per molecule is difficult. The fractions of loops and chains of a given length that have different d and m characteristics is, however, theoretically more tractable. A simple model, which accounts for the entropy associated with the number of ways that the chain can be connected, reproduces the results for pure water [9]. Since this entropic term is independent of x_{MeCN}, one must consider other mechanisms to account for the change in $\langle d \rangle$. The average directionality of shorter loops, in contrast to chains, is essentially independent of x_{MeCN}. There are indications that short loops with one or two meeting points (which would infer low directionality) have low potential energy [9]. High loop directionality would thus be correlated with high potential energy, which would render the loop directionality less sensitive to changes in x_{MeCN}.

VIII. CONCLUSION

We have approached the structure of the water-acetonitrile mixture in three stages. First, the average spatial structure has been studied using RDF's and SDF's. The RDF's show that there is a strong tendency for the water molecules to aggregate and form clusters. The SDF's show that, apart from the dominant hydrogen-bond coordination, there is an alternative type of coordination of both oxygen and nitrogen atoms at nontetrahedral positions.

Second, we have studied basic hydrogen-bond properties using the effective hydrogen-bond definition. The average number of HN and HO bonds have been computed. The number of HN bonds agrees reasonably with experimental predictions, but the number of HO bonds at high acetonitrile concentrations differs significantly. The causes of the discrepancy are unknown. We have also found that the average lifetime of the hydrogen bonds increases with the acetonitrile concentration. A possible explanation is the lack of competition between the water molecules.

Third, we have analyzed the structure of the hydrogen-bond network. The network surrounding a water molecule depends on the number of acetonitrile molecules that it binds to: Water molecules that bind to one acetonitrile molecule are as strongly incorporated in the water network as those that bind to none. Water molecules binding to two acetonitrile molecules are, however, more weakly incorporated in the water network. The topology of the hydrogen-bond network changes as the acetonitrile concentration increases: The number of loops per molecule decreases, the maximum is shifted from six to five loops, and the directionality of chains increases. These local changes are accompanied by a global breakdown of the infinite network of connected water molecules at a critical acetonitrile concentration between 0.11 and 0.5.

Our results do not fully characterize the structure of the water-acetonitrile mixture. Several important questions regarding the microheterogeneities proposed by Moreau and Douhéret remain. A simulation of a larger system could answer some of these questions. We expect our approach to be useful when analyzing such a simulation. The approach can also be useful when studying other liquid mixtures where hydrogen bonds are an important mode of interaction [28,35,36].

ACKNOWLEDGMENTS

This work has been supported by the Swedish Natural Science Research Council (NFR). The simulations have been carried out at the Center for Parallel Computers at The Royal Institute of Technology.

[1] M. Moolel and H. Schneider, Z. Phys. Chem. (Munich) **74**, 237 (1971).

[2] G. Benter and H. Schneider, Ber. Bunsenges. Phys. Chem. **77**, 997 (1973).

[3] K. W. Morcom and R. W. Smith, J. Chem. Thermodyn. **1**, 503 (1969).

[4] C. Moreau and G. Douhéret, Thermochim. Acta **13**, 385 (1975); J. Chem. Thermodyn. **8**, 403 (1976); G. Douhéret, C.

Moreau, and A. Viallard, Fluid Phase Equilibria **22**, 289 (1985).
[5] D. Jamroz, J. Stangret, and J. Lindgren, J. Am. Chem. Soc. **115**, 6165 (1993).
[6] J. E. Bertie and Z. Lan, J. Phys. Chem. B **101**, 4111 (1997).
[7] H. Kovacs and A. Laaksonen, J. Am. Chem. Soc. **113**, 5596 (1991).
[8] D. Bergman and A. Laaksonen, Mol. Simul. **20**, 245 (1998).
[9] D. L. Bergman (unpublished).
[10] M. G. Sceats and S. A. Rice, in *Water: A Comprehensive Treatise*, edited by F. Franks (Plenum Press, New York, 1982), Vol. 7, pp. 160–211.
[11] H. E. Stanley, J. Teixeira, A. Geiger, and R. L. Blumberg, Physica A **106**, 260 (1981); A. Geiger and H. E. Stanley, Phys. Rev. Lett. **49**, 1749 (1982); R. L. Blumberg, H. E. Stanley, A. Geiger, and P. Mausbach, J. Chem. Phys. **80**, 5230 (1984).
[12] M. Matsumoto and I. Ohmine, J. Chem. Phys. **104**, 2705 (1996).
[13] A. Rahman and F. H. Stillinger, J. Am. Chem. Soc. **95**, 7943 (1973).
[14] H. E. Stanley, R. L. Blumberg, and A. Geiger, Phys. Rev. B **28**, 1626 (1983).
[15] T. P. Radhakrishnan and W. C. Herndon, J. Phys. Chem. **95**, 10 609 (1991).
[16] I. Okabe, H. Tanaka, and K. Nakanishi, Phys. Rev. E **53**, 2638 (1996).
[17] W. L. Jorgensen and J. M. Briggs, Mol. Phys. **63**, 547 (1988).
[18] H. J. C. Berendsen, J. R. Grigera, and T. P. Straatsma, J. Phys. Chem. **91**, 6269 (1987).
[19] We have used the experimental densities measured at $T = 298.15$ K and $p = 1.013 \cdot 10^5$ pa [4].
[20] M. Allen and D. J. Tildesley, *Computer Simulation in Liquids* (Oxford University Press, Oxford, 1989).
[21] P. P. Ewald, Ann. Phys. (Leipzig) **64**, 253 (1921).
[22] A. Laaksonen, Comput. Phys. Commun. **42**, 271 (1986).
[23] H. G. Hertz and H. Leiter, Z. Phys. Chem. (Munich) **133**, 45 (1982).
[24] We have developed the program package TOP-PACK in order to generate graphs and to analyze them from a topological point of view.
[25] I. M. Svishchev and P. G. Kusalik, J. Chem. Phys. **99**, 3049 (1993).
[26] All SDF's can be obtained from ftp://ftp.fos.su.se/pub/documents/dan/acetonitrile-water/
[27] F. H. Stillinger, Science **209**, 451 (1980).
[28] M. Mezei and D. L. Beveridge, J. Chem. Phys. **74**, 622 (1981).
[29] It is not meaningful to use a g_c value smaller than 1.3, since the volumes defining the hydrogen-bond sites would no longer be small and shaped as in Fig. 3(c).
[30] We discard oxygen before nitrogen atoms, and if two atoms of the same kind overlap then we randomly discard one of them.
[31] We have used the strict criterion to define the hydrogen bonds when we estimate the lifetimes. This ensures that two atoms never enter the same hydrogen-bond site simultaneously.
[32] According to the strict definition.
[33] Alexander Lyubartsev has suggested that a lower bound on the lifetime can be obtained by defining the bond as terminated when the original atom leaves the site for the last time.
[34] M. A. Armstrong, *Basic Topology* (Springer-Verlag, New York, 1983).
[35] K. Koga and H. Tanaka, J. Chem. Phys. **104**, 263 (1996).
[36] R. M. Lynden-Bell and J. C. Rasaiah, J. Chem. Phys. **107**, 1981 (1997).